Oncogene (2009) 28, 973–982

www.nature.com/onc

ORIGINAL ARTICLE

Menin interacts with IQGAP1 to enhance intercellular adhesion of β-cells

J Yan[1], Y Yang[1], H Zhang[1,2], C King[1], H-M Kan[3], Y Cai[3], C-X Yuan[4], GS Bloom[3,5] and X Hua[1]

[1]*Department of Cancer Biology, Abramson Family Cancer Research Institute, University of Pennsylvania School of Medicine, Philadelphia, PA, USA;* [2]*Zhongshan Ophthalmic Center, Sun Yat-sen University, Guangzhou, China;* [3]*Department of Biology, University of Virginia, Charlottesville, VA, USA;* [4]*Department of Proteomic Facility, University of Pennsylvania School of Medicine, Philadelphia, PA, USA and* [5]*Department of Cell Biology, University of Virginia, Charlottesville, VA, USA*

Multiple endocrine neoplasia type 1 (MEN1) is a dominantly inherited tumor syndrome that results from the mutation of the *MEN1* gene that encodes protein menin. Stable overexpression of *MEN1* has been shown to partially suppress the Ras-mediated morphological changes of fibroblast cells. Little is known about the molecular mechanisms by which menin decreases the oncogenic effects on cell morphology and other phenotypes. Here we showed that ectopic expression of menin in pretumor β-cells increases islet cell adhesion and reduces cell migration. Our further studies revealed that menin interacts with the scaffold protein, IQ motif containing GTPase activating protein 1 (IQGAP1), reduces GTP–Rac1 interaction with IQGAP1 but increases epithelial cadherin (E-cadherin)/β-catenin interaction with IQGAP1. Consistent with an essential role for menin in regulating β-cell adhesion *in vivo*, accumulations of β-catenin and E-cadherin are reduced at cell junctions in the islets from *Men1*-excised mice. Together, these results define a novel menin–IQGAP1 pathway that controls cell migration and cell–cell adhesion in endocrine cells.
Oncogene (2009) **28,** 973–982; doi:10.1038/onc.2008.435; published online 15 December 2008

Keywords: menin; IQGAP1; intercellular adhesion; migration

Introduction

Multiple endocrine neoplasia type 1 (MEN1) is a dominantly inherited tumor syndrome that results from the mutation of *Men1* (Chandrasekharappa *et al*., 1997), which encodes menin protein. Menin has been found to interact with mixed lineage leukemia (MLL) protein (Hughes *et al*., 2004), which is a histone H3 lysine 4 (H3K4) methyltransferase (Milne *et al*., 2002). Multiple lines of evidence indicate that one of menin's biochemical functions is to promote MLL-dependent H3K4 methylation, leading to enhanced transcription of target genes such as *Hoxa9* and cyclin-dependent kinase inhibitors, p18 and p27 (Milne *et al*., 2005; Yokoyama *et al*., 2005; Chen *et al*., 2006; Yan *et al*., 2006a). However, it is not clear why the attenuated menin expression specifically causes a unique and restricted pattern of endocrine tumors in both humans and mice despite the ubiquitous expression of menin in almost all tissues (Guru *et al*., 1999).

Men1$^{-/-}$ mice die in mid gestation (between embryonic days 11.5 and 13.5), whereas *Men1*$^{+/-}$ mice develop endocrine tumors later in their life with a spectrum similar to that in MEN1 patients (Crabtree *et al*., 2001). Heterogeneous expression of *Men1* suggests that attenuation, rather than complete abrogation of *Men1* function, facilitates a tumorigenic signaling pathway in endocrine cells (Crabtree *et al*., 2003). Although conditional alleles have been generated to allow tissue-specific homozygous deletion of *Men1* (Schnepp *et al*., 2006), *Men1*$^{+/-}$ mice, presumably retaining a lower level of menin expression, were used to gain an unbiased assessment of the functional *in vivo* interaction between menin with p18 and p27 proteins (Bai *et al*., 2007).

An alternate approach to evaluate *Men1*-mutation phenotype is to use neoplastic cells transformed by oncogenes. *Ras* is an oncogene originally identified in rat sarcoma virus. Transforming *Ras* genes cause tumor progression, often accompanied by somatic mutations in tumor suppressor genes (Jiang *et al*., 2004). Through this approach, Kim *et al*. (1999) first demonstrated that stable overexpression of *Men1* partially suppressed the *Ras*-mediated tumor phenotype in NIH 3T3 fibroblast cells. However, little is known about the molecular mechanisms by which menin decreases the oncogenic effects upon cell morphology.

To address menin's role in endocrine cells, we sought to test menin's tumor suppressing function by ectopic expression of menin in βHC9 pretumor β-cells. This cell line was generated from individual hyperplastic pancreatic islets (a tumor precursor stage) of transgenic mice expressing the SV40 large T antigen under control of the rat insulin promoter (Radvanyi *et al*., 1993). Using this cell model, we found that ectopic menin expression increased cell adhesion and promoted normal endocrine cell morphology. Menin interacted with a scaffold protein, IQ motif containing GTPase activating protein 1 (IQGAP1) and attenuated GTP–Rac1 binding

Correspondence: Dr X Hua, Department of Cancer Biology, Abramson Family Cancer Research Institute, University of Pennsylvania School of Medicine, 421 Curie Boulevard, Philadelphia, PA 19104, USA.
E-mail: huax@mail.med.upenn.edu
Received 2 April 2008; revised 10 October 2008; accepted 1 November 2008; published online 15 December 2008

to IQGAP1 but enhanced binding of epithelial cadherin (E-cadherin)/β-catenin to IQGAP1. Immunostaining showed that E-cadherin and β-catenin were reduced at cell junctions in the islets of *Men1*-excised mice. These results define a novel menin–IQGAP1 pathway that links the cytoskeleton to cell adhesion and migration in endocrine cells.

Results

Menin enhances aggregation of islet cells

To investigate the function of menin in islet β-cells, we ectopically expressed menin in an insulin-secreting β-cell line, βHC9. More specifically, βHC9 cells were infected with either control recombinant retroviruses or retroviruses expressing menin tagged with the tandem-affinity purification (TAP) epitopes, streptavidin-binding peptide (SBP) and calmodulin-binding peptide (Supplementary data, Supplementary Figure S1A). The resulting pooled and menin-expressing retrovirus-infected cells (Men1-TAP) showed approximately 2 to 3-fold higher menin expression, with the size of the tagged menin slightly bigger than the endogenous menin, as compared with the vector-infected control cells (mock) based on immunoblotting (Supplementary Figure S1C). High-density Men1-TAP cells but not control cells formed multilayers of cell clusters and thus more closely mimicked normal islet morphology (Figures 1a and b). At a low density, control cells were well spread and separated from each other, and readily formed lamellipodia (Figure 1c). In contrast, low-density Men1-TAP cells were relatively round and formed compact clusters, but not lamellipodia (Figure 1d). The polarized appearance that distinguished individual control cells from Men1-TAP cells were defined by cell shape index, that is 2.5 ± 0.5 versus 1 ± 0.1 ($n = 10$; $\pm$s.d.; see Figure 1 legend).

To test the possibility that the epitope tags fused with menin, rather than ectopic menin expression, contributed to the morphological changes, we generated an additional stable cell line by infecting βHC9 cells with retroviruses expressing untagged menin (Supplementary Figure S1A). The resulting cell line (Men1), showed a higher level of menin expression (Supplementary Figure S1C, lane 3), and a more compact, clustered phenotype as compared to control, vector-infected cells (Supplementary Figure S1B).

Menin expression changes actin distribution

The morphological changes described above were likely to reflect changes in cytoskeletal organization, particularly of actin filaments. Although stress fibers were rarely seen in both cell types, more F-actin patches were found in the cytoplasm of mock-infected control cells than Men1-TAP cells. The other conspicuous difference in actin organization between the two cell types was the accumulations of F-actin surrounding the cell membrane of Men1-TAP versus at the leading edge of control cells (Figures 1e–h). The distribution difference was reflected by a $\sim$50% loss of β-actin in menin-overexpressing cells, as determined by immunobloting

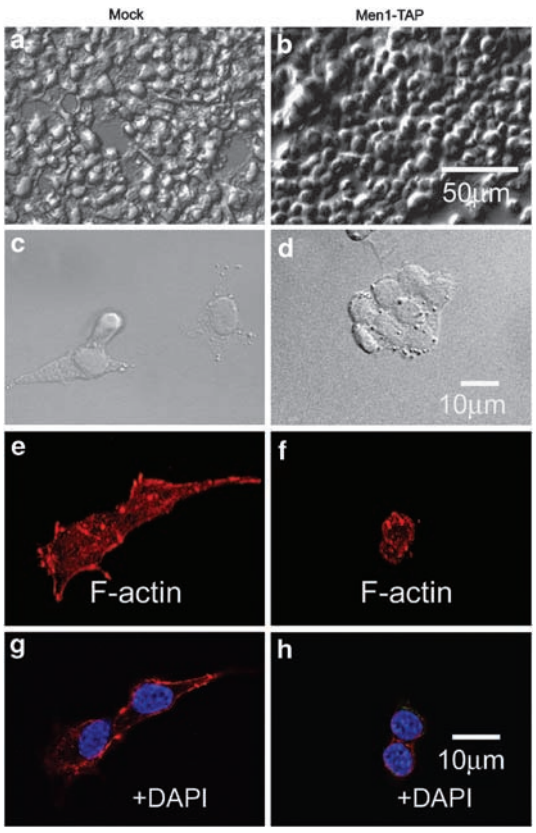

Figure 1 Menin overexpression induces βHC9 cells to become compact and clustered. Two types of βHC9-derived cell lines are shown: mock (pMX-puro empty vector) and *Men1* tandem-affinity purification (TAP; overexpressing menin-TAP). Differential interference contrast images of cells are shown at low (**a** and **b**) and high (**c** and **d**) magnification. Texas Red-phalloidin staining was used to assess the organization of F-actin. Eleven confocal Z-stacks were taken and projected into one image (**e** and **f**), and a single confocal section stained for F-actin and for nuclei with 4′-,6-diamidino-2-phenylindole is also shown (**g** and **h**). The morphological polarity of a cell was defined by a seminquantitative index of cell shape as described by Donnadieu *et al*. (1992). Briefly, the cell was traced as an ellipse using Photoshop software. Two lines were drawn: one along the longest axis of the ellipse; the other perpendicular to the first and bisecting it. The cell shape index was determined by the ratio of the long axis to the short axis.

(Figure 2d) and quantitative real-time PCR (data not shown). These results suggest that menin expression promotes actin assembly at cell membrane and negatively regulates steady state levels of β-actin in cytoplasm, possibly because of delocalization of IQGAP1 (see below).

Menin interacts with IQGAP1

During our investigation into the role of menin in controlling cell morphology, we tried to identify menin interacting proteins in β-cells. To that end, we subjected the mock cells and Men1-TAP cells to sequential affinity purifications, using streptavidin- and calmodulin-conjugated beads. One major band at $\sim$180 kDa was reproducibly identified during multiple rounds of purification in Men1-TAP cells, but not in the mock cells, indicating specific association with the tagged menin (Figure 2a).

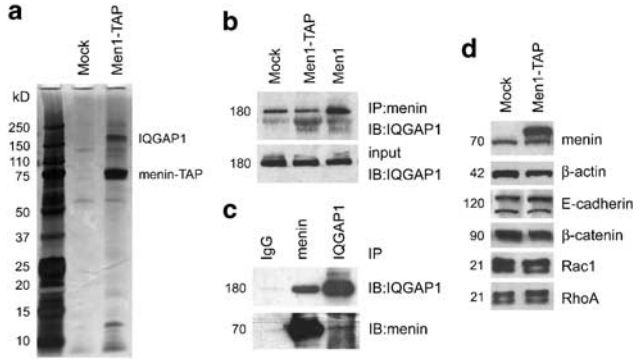

Figure 2 IQ motif containing GTPase activating protein 1 (IQGAP1) is a major cytoplasmic-binding partner of menin. Soluble extracts from mock cells and *Men1* tandem-affinity purification (TAP) cells were used for TAP purification. (**a**) The purified products were separated on SDS–polyacrylamide gel electrophoresis (PAGE) and identified with silver staining. The two most prominent bands in lane 3 were excised from the gel, and their tryptic peptides were identified as menin and IQGAP1 by mass spectrometry (nanoLC/nanospray/MS/MS). (**b** and **c**) Physical interactions between menin and IQGAP1 were verified by *in vitro* reciprocal immunoprecipitation. (**d**) Comparative expression levels of proteins marked by the indicated antibodies in mock and Men1-TAP cells.

Mass spectrometry identified this band as IQGAP1, a scaffold protein that interacts with a variety of proteins, including Rac1, Cdc42, E-cadherin, β-catenin and F-actin to regulate cell motility and adhesion (Fukata *et al*., 1999; Lambert *et al*., 2002; Mataraza *et al*., 2007).

Physical interaction between menin and IQGAP1 was confirmed by a coimmunoprecipitation (IP) assay. An antimenin antibody was able to pull-down IQGAP1 in both mock-infected and menin-overexpressing cells (Figure 2b), and more IQGAP1 was present in antimenin IPs obtained from Men1 cells than from control cells (Figure 2b). The latter result suggested that IQGAP1 interacted with both endogenous and ectopically expressed menin. We noticed, however, that the amount of IQGAP1 in IPs obtained from mock and Men1-TAP cells were nearly identical, despite the large presence of menin in the Men1-TAP cells (Figures 2b and d). This is likely because of the fact that the immunoprecipitating anti-menin antibody (BL342) was generated using a synthetic peptide corresponding to the C terminus of human menin and thus may have had a lower affinity for menin modified at its C terminus with the TAP epitope tag than for unmodified menin. Reciprocal co-IP experiments demonstrated that anti-IQGAP1 (Mateer *et al*., 2002) could pull-down menin (Figure 2c), albeit less effectively than antimenin pulled down IQGAP1 (Figure 2b). This result suggests that either a small fraction of menin binds IQGAP1 or the affinity between menin and IQGAP1 is negatively affected by the anti-IQGAP1 antibody. In either case, these collective results indicate that menin and IQGAP1 interact in β-cells.

Menin increases IQGAP1 accumulation at the plasma membrane

Consistent with our biochemical evidence for an IQGAP1–menin association in cells (Figures 2a–c), we found extensive immunofluorescent colocalization of IQGAP1 with a nonnuclear pool of menin in our β-cell lines. However, colocalization around the plasma membrane appeared more extensive in Men1-TAP cultures than in controls, especially at cell–cell junctions (Figure 3a). The impression that menin overexpression enhanced IQGAP1 localization at the cell surface was further supported by transient transfection studies of IQGAP1-yellow fluorescent protein (YFP). Cortical enrichment of the fluorescent fusion protein was much more evident in the Men1-TAP cells than in control cells (Figure 3b). Interestingly, coexpression of mCherry-Rac1 with IQGAP1-YFP prevented the overexpressed menin in Men1-TAP cells from targeting IQGAP1 to the cortex (Figure 3c). As expected, overexpression of mCherry-Rac1 increased the level of Rac1–GTP, an active form to bind IQGAP1 (Supplementary Figure S3). These results suggest that the intracellular distribution of IQGAP1 is controlled by both menin and Rac1, but that Rac1 is dominant.

Menin increases accumulation of E-cadherin/β-catenin at cell–cell contact sites

Having established the intracellular distributions of menin and IQGAP1, we next investigated the biological significance of menin-induced IQGAP1 accumulation at intercellular adhesion sites. As determined by cell adhesion assays (Price *et al*., 2004), cells expressing menin (Men1) had strong adhesion, particularly to Fc-E-cadherin (Figure 4a). By immunofluorescence, E-cadherin was 2–3 times more concentrated at sites of cell–cell contact in menin-expressing cells than anywhere along the surfaces of mock-infected control cells (Figure 4c). The distribution of β-catenin was similar to E-cadherin staining in βHC9-derived cells. Menin-expressing cells displayed broader bands of β-catenin staining, reflecting regions of cellular contact (Figure 4c). In mock cells, however, β-catenin was frequently restricted to a thin line where adjacent mock cells made contact, and showed a 2 to 3-fold of lower staining intensity than in menin-expressing cells (Figure 4c). Immunoblots of cell lysates revealed comparable levels of E-cadherin and β-catenin in the mock and Men1-TAP cell lines (Figure 2d). Together, these results suggest that menin-expression significantly increased intercellular adhesion by E-cadherin pathway.

To examine whether distributions of β-catenin and E-cadherin are altered in Men1-associated islet tumors, we immunostained enlarged islets from the *Men1*-excised mice and control islets from wild-type mice (Schnepp *et al*., 2006). As shown in Figure 4d, the staining intensity of E-cadherin surrounding the cell membrane was much higher in menin-expressing control islets. In the case of β-catenin, staining intensity was very similar in the control and *Men1*-excised mice, but β-catenin labeling was confined to a narrower band near the surface of Men1 knockout islet cells. These regions of β-catenin immunoreactivity ranged from 0.5 to 2 μm wide in Men1-deleted islet cells but were 2–4 μm wide in control islets. These results suggest that Men1-deletion leads to reduced distribution of E-cadherin and β-catenin at the surface of pancreatic islet cells.

To demonstrate the association of menin and IQGAP1 with cadherin complex, Men1 cells and IQGAP1 short-hairpin RNA (shRNA)-expressing cells were subjected to IP with anti-menin antibody, followed by western blotting with either anti-β-catenin or anti-IQGAP1 antibodies. IQGAP1 and β-catenin were simultaneously immunoprecipitated by menin-specific antibodies. At similar amount of β-catenin input, the

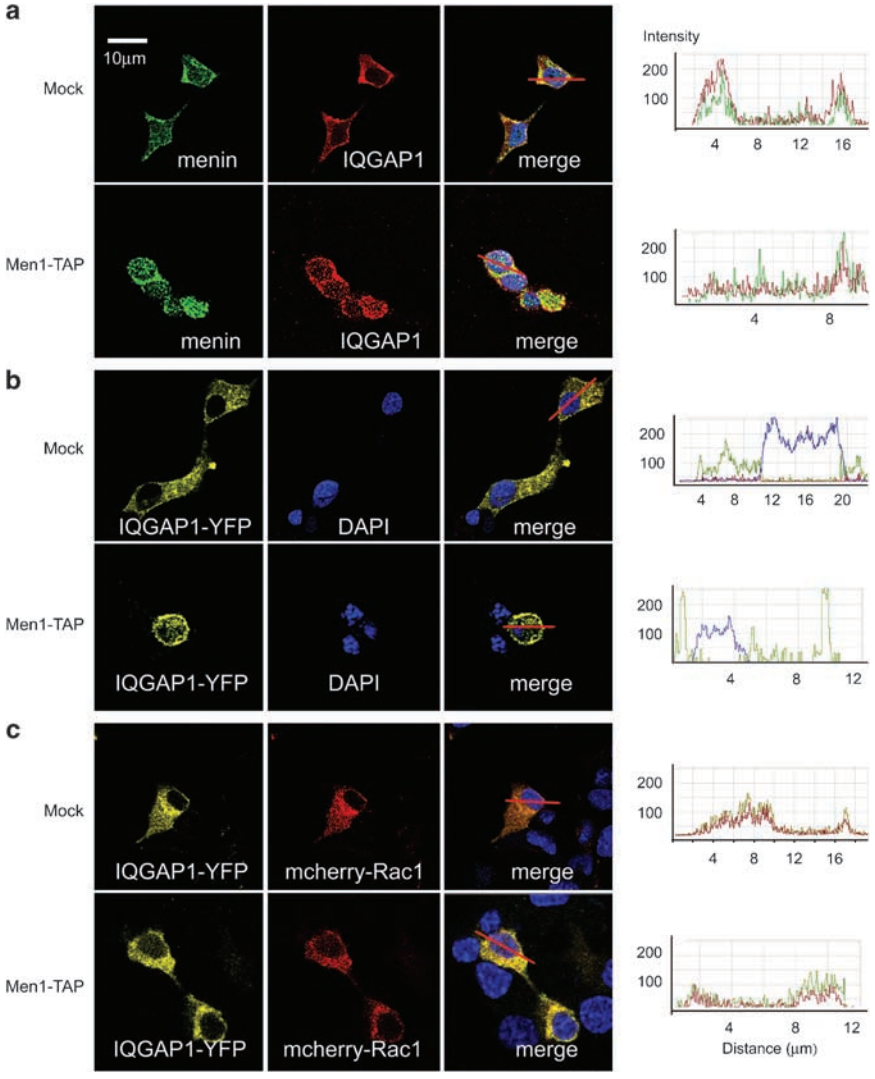

Figure 3 Menin colocalizes with IQ motif containing GTPase activating protein 1 (IQGAP1) in β-cell lines. The right panel showed quantitative analyses of fluorescence intensity across colocalized areas using Zeiss LSM510 software, underscoring the fluorescence distribution in the membrane and cytoplasm (that is peak's breadth). (**a**) Distinct enrichments of menin at the cell–cell contacts in mock and *Men1* tandem-affinity purification (TAP) cells. (**b**) Distinct accumulations of overexpressed IQGAP1-yellow fluorescent protein (YFP) on the cell surface and in the cytoplasm between mock and Men1-TAP cell. (**c**) Overexpressed mCherry-Rac1 delocalizing subcellular distributions of IQGAP1-YFP in Men1-TAP cells.

Figure 4 Menin promotes cell–cell adhesions. (**a**) Cells were detached with 1.5 mM ethylenediaminetetraacetic acid phosphate-buffered saline (PBS) at 37 °C for either 5 min (mock) or 15 min (Men1). The detached cells were diluted and added to wells coated with PBS, fibronectin or Fc-E-cadherin (E-cad). The number of adherent cells per microscopic field is presented ($n=5$; ± s.d.). (**b**) IQ motif containing GTPase activating protein 1 (IQGAP1) knockdown reduced cell adhesion to E-cadherin in menin overexpression cells. Men1 cells were infected with either IQGAP1 short-hairpin RNA (shRNA) or scramble shRNA lentiviruses, followed by adhesion assays ($n=8$; ± s.d.). Two tailed *t*-test was used to determine the *P*-value for the difference as shown in the figure. Intercellular junctions marked by E-cadherin and β-catenin in βHC9-derived cell lines (**c**) and paraffin-embedded islets from wild-type or *Men1*$^{+/-}$ mice (**d**) were imaged by immunofluorescence. Quantitative analyses of fluorescence intensity across long linear paths that intersect with at least three cell–cell contacts were performed using Zeiss LSM510 software. (**e**) Detection of menin, IQGAP1 and β-catenin complex. IQGAP1 was knocked down with a pool of five lentiviral shRNA constructs against murine IQGAP1. The cell lysates from control or IQGAP1 shRNA knockdown Men1 cells were immunoprecipitated with menin-specific antibodies, followed by western blotting to determine the association of IQGAP1 and β-catenin with menin. The bottom histogram shows quantification of β-catenin in lysate and menin-immunoprecipitation from control and IQGAP1-deficient cells as in (**b**), normalized by β-catenin level in control lysate. *Paired *t*-test, $P<0.05$.

levels of β-catenin were reduced by ~60% in IPs obtained from IQGAP1 knockdown cells (Figure 4e). Furthermore, IQGAP1-deficient cells reduced staining intensity of E-cadherin and β-catenin at the cell–cell contacts (Supplementary Figure S4), and displayed a weak cell adhesion (Figure 4b). Thus, IQGAP1 is crucial to bridge the menin E-cadherin/β-catenin interactions in islet cells.

Menin expression inhibits β-cell migration

To assess the importance of the menin–IQGAP1 interaction in β-cell motility, we performed a modified Boyden

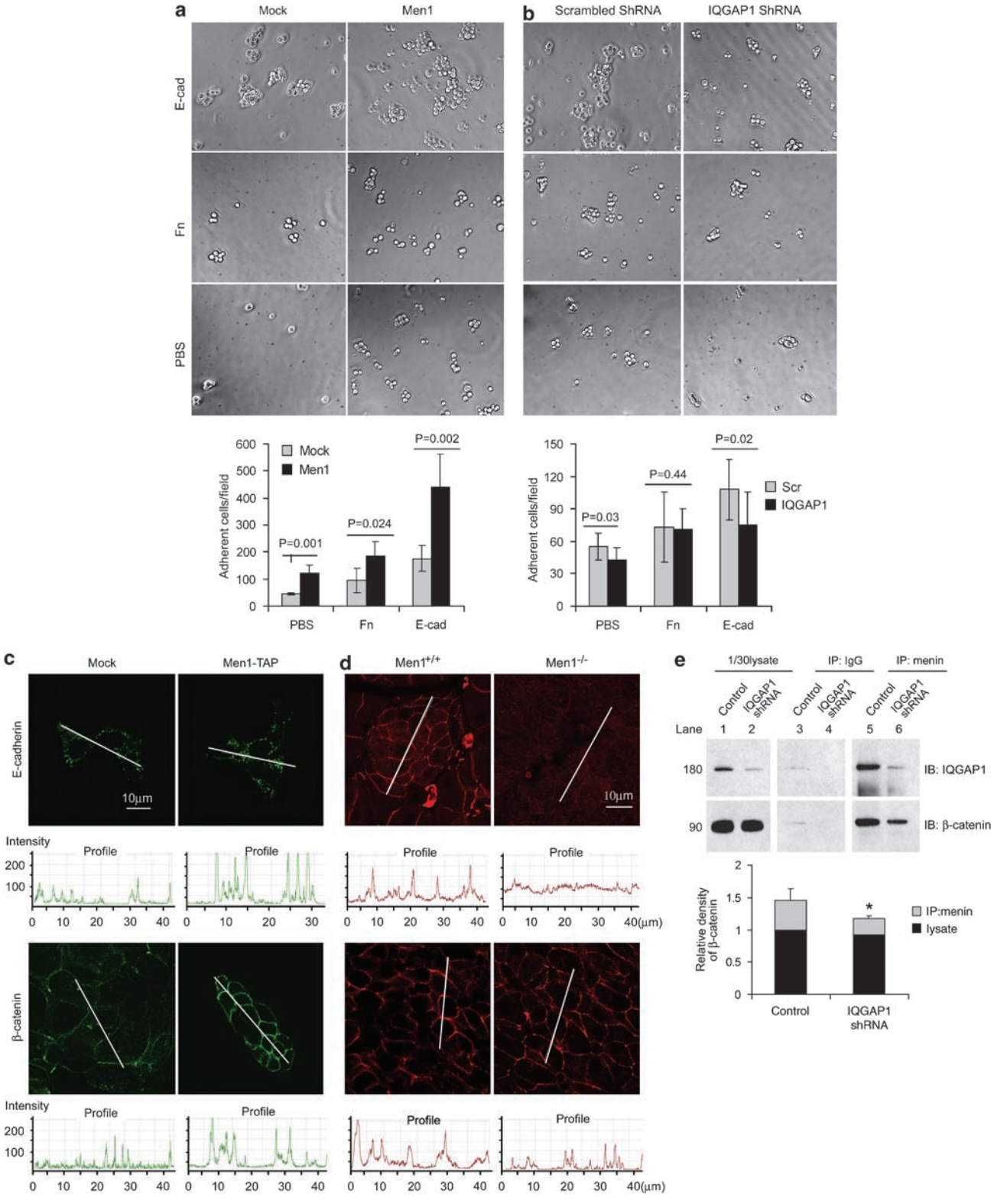

chamber assay. After 24 h of migration, virtually all of the Men1-TAP cells remained in the upper chamber, but a small number of mock cells migrated completely through the filter membrane (Figure 5A). Because the total number of migratory and nonmigratory mock cells was less than that of the seeded cells, we suspected that quite a number of mock cells might be trapped in the filter membrane. We therefore used an alternative approach, the scratch wound assay, to compare the motility of mock versus Men1-TAP cells. As can be seen in Figure 5B, the degree of wound closure achieved by mock cells within 24 h of wounding was comparable to what was seen after 5 days by the Men1-TAP cells. The dramatic difference between the two cells lines reinforces the impression from the Boyden chamber migration assays that menin overexpression reduces cell motility.

To test the effect of Rac1 activity on menin inhibition of cell mobility, we transiently overexpressed constitutively active mutant, RFP-Rac1 (Q61L) in Men1-TAP cells. After 24 h, Men1-TAP cells reduced the wound gap by 13% (64 μm out of 511 μm) relative to 53% (276 μm out of 519 μm) of mock control cells (Supplementary Figure S5). However, overexpression of active Rac1 (Q61L) increased the migration speed of Men1-TAP cell twofold from 64 to 122 μm (Supplementary Figure S5). Thus, active Rac1 can abrogate the migratory inhibition caused by Men1 expression in β-cell.

Menin modulates IQGAP1 interactions with Rac1

IQGAP1 has been reported to promote cell motility by interactions with Rac1 and Cdc42 (Bensenor *et al*., 2007; Mataraza *et al*., 2007). To test whether menin affects the IQGAP1–Rac1 interaction, we performed affinity pull-down assays to examine associations of menin, IQGAP1 and Rac1 (Supplementary Figure S6A). We precoated Ni-NTA agarose with His-tagged IQGAP1 and then subsequently incubated the coated beads with menin and activated or inactive Rac1. As expected, menin and GTPγS-Rac1 bound independently to IQGAP1 (lanes 4 and 6). The affinity of GDP-Rac1 to IQGAP1 was very low, slightly higher than its background binding to naked Ni-NTA agarose beads (lane 5 versus lane 2). However, GTPγS-Rac1 binding to IQGAP1 was substantially reduced in the presence of menin (lane 7). Thus, activated Rac1 and menin may competitively bind to IQGAP1. This conclusion was fortified by studies of live cells. Mock cells and menin-overexpressing cells were subjected to IPs and immunoblotting. Anti-Rac1 pulled down IQGAP1 but 2.8-fold less effectively in cells that ectopically expressed menin (Supplementary Figure S6B and C).

To determine regions in IQGAP1 responsible for menin binding, we tested menin binding to various recombinant fragments of IQGAP1. In these assays, menin showed a weak interaction with N-terminal fragment IQGAP1-N2 (aa 2–522) and strong binding to C-terminal fragments including IQGAP1-C3 (aa 956–1657). However, C3-splited shorter fragment C1 (aa 956–1274) and C2 (aa 1276–1657) did not bind or displayed a weak interaction to menin (Figures 6a–c). Together with a previous study showing direct interactions between C1, C2 and N2 (Grohmanova *et al*., 2004; Le Clainche *et al*., 2007), our data suggest that the binding of menin to IQGAP1 depends on the tertiary structure formed between the C-terminal (C3) and N-terminal (N2) domains. Menin–IQGAP1 structural binding may induce IQGAP1 C-terminal conformation affinity toward E-cadherin/β-catenin but against Rac1–GTP (Figure 6e).

Menin expression reduces Rac1–GTP

Small GTPases of the Rho family, including Rac1, RhoA and Cdc42, regulate multiple signaling pathways that affect cell shape and motility, transcription, and cell cycle progression (Ridley, 2001). Thus, we sought to determine whether menin affects the activities of these small G proteins using assays to measure their binding to partners that selectively interact with GTP-bound forms of Rac1, RhoA or Cdc42 (Taylor and Shalloway, 1996). Before harvesting the cells for GTPase-binding assays, the cells were serum starved and then stimulated with fresh serum. As shown in Figure 6d, menin overexpression caused a dramatic suppression of Rac1 activation by serum stimulation.

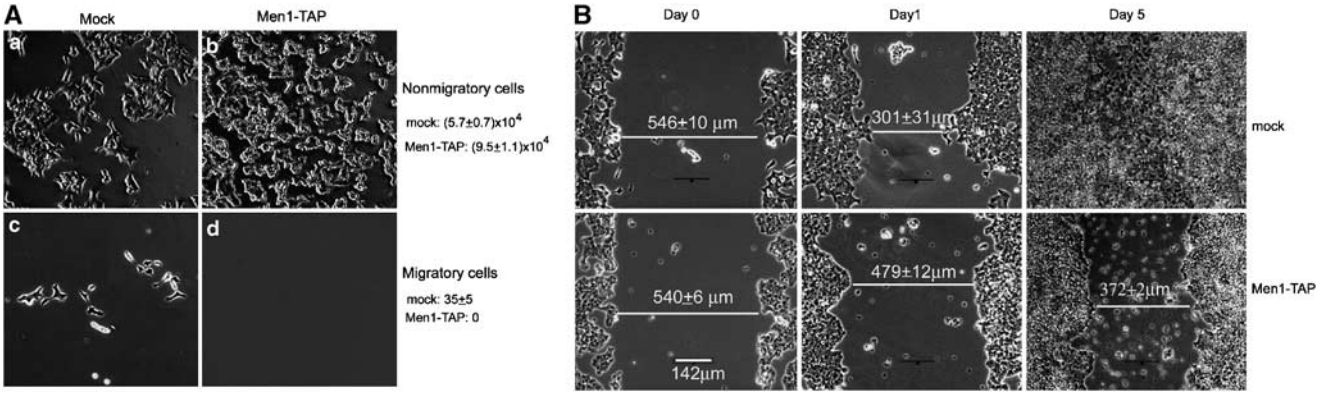

Figure 5 Menin inhibits migration of βHC9-derived cells. (**A**) An equal number of mock cells or Men1 tandem-affinity purification cells were seeded onto the upper chamber and 24 h later. Cells that remained in the upper chamber and those moved to the lower surface of the filter membrane were photographed and counted. (**B**) Menin overexpression inhibited closure of artificial wounds made in confluent cellular monolayers. One of three assays was shown ($n = 3$; ± s.d.).

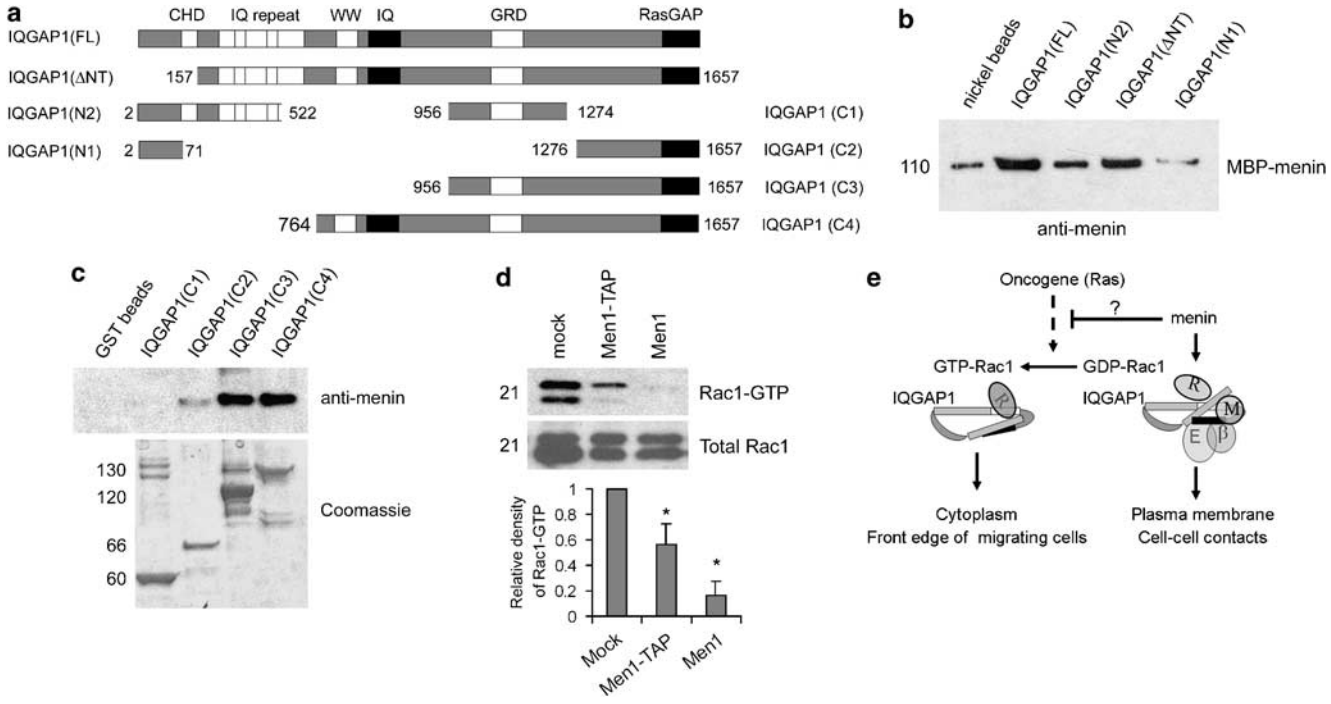

Figure 6 Menin directly binds to IQ motif containing GTPase activating protein 1 (IQGAP1). (**a**) A schematic diagram of functional domains present in full-length IQGAP1 and seven fragments used for binding assays. (**b**) Nickel-agarose beads were precoated with 2 μg of His-tagged IQGAP1 (FL), IQGAP1 (ΔNT), IQGAP1 (N2), IQGAP1 (N1) or bovine serum albumin as a negative control. The precoated beads were then incubated 0.2 μg of menin. Chemiluminescent immunoblotting was used to detect any menin that may have bound to beads. (**c**) Precoated glutathione *S*-transferase (GST)-fusion C-terminal proteins of IQGAP1 were incubated with menin (0.2 μg). Top: antimenin western blot of bound menin. Bottom: Coomassie stained gel slices show input of the GST-fusion proteins. Comparison of western blot and Coomassie staining indicated that all samples of precoated GST-fusions were saturated over menin binding. (**d**) Menin overexpression reduces cellular levels of activated Rac1. PAK1-PBD agarose and Rhotekin RBD agarose were used to isolate GTP–Rac1 from whole cell lysates from each of the indicated cell lines. The collected complexes were then resolved by SDS–polyacrylamide gel electrophoresis (PAGE), and probed with an anti-Rac1 antibody. The amount of Rac1–GTP was quantified by densitometry and normalized by the total input Rac1 protein. Relative to mock cells, Rac1–GTP reduced twofold and sixfold in Men1-TAP and Men1 cells, respectively. *Paired *t*-test, $P<0.05$. (**e**) A model for menin-regulated IQGAP interaction with the Rac1 and E-cadherin/β-catenin complex. When membrane menin increases, menin inhibits Rac1 activation and binds the tertiary structure by folding the C terminus (C1 and C2) and N terminus (N2) of IQGAP1. Their bindings induce IQGAP1 conformation switch to E-cadherin/β-catenin binding (black box, RasGAP domain) at cell–cell contacts and enhance intercellular adhesion. When reduction of menin activity occurs in tumor cells by *Men1* mutation, or increase of Rac1 activity by oncogene, such as *Ras*, Rac1–GTP interacts with IQGAP1 (blank box, GRD domain) and increases IQGAP1 accumulations in cytoplasm and at the front edge of migrating cells, thereby promoting cell mobility.

RhoA-GTP level was increased but not consistent in mock cells, suggesting that RhoA may play a complicate function in β-cells (Supplementary Figure S6D). Neither Cdc42-GTP nor total Cdc42 were detected in these cell lines (Supplementary Figure S6D and E). Collectively, these results indicate that Rac1 is a major Rho family GTPase in the islet cell lines used for this study, and that menin potently prevents Rac1 activation. Inactivation of Rac1 is possibly another mechanism by which menin competitively inhibits Rac1–IQGAP1 interaction in living cells (Figure 6e).

Discussion

Menin mutations have been known for more than a decade to cause the MEN1 class of multiple endocrine tumors (Chandrasekharappa *et al*., 1997), but the oncogenic mechanisms have remained obscure. Until recently, most studies of menin have focused on its role in the nucleus, where it indirectly regulates histone H3 methylation and transcription of at least a few genes that are involved in cell cycle control (Milne *et al*., 2002, 2005; Schnepp *et al*., 2006). Although menin is primarily a nuclear protein, it is also detectable in the cytoplasm and on membranes (Guru *et al*., 1998), and its differential distribution between the nucleus and cytoplasm is cell cycle dependent (Huang *et al*., 1999; Lopez-Egido *et al*., 2002). Because little is known about the function of cytoplasmic menin in β-cells, we decided to search for cytoplasmic-binding partners of menin. We found that a major cytoplasmic-binding partner of menin is IQGAP1 (Figure 2), a protein known to be intimately involved in controlling cellular motility and morphogenesis through regulation of actin assembly (Bensenor *et al*., 2007; Brandt *et al*., 2007; Le Clainche *et al*., 2007) and intercellular adhesion (Kuroda *et al*., 1998). We propose a menin–IQGAP1 pathway, which contrasts and complements the 'menin–MLL pathway' in the nucleus (Hughes *et al*., 2004; Yokoyama *et al*., 2005; Chen *et al*., 2006; Yan *et al*., 2006a).

Functional interaction between menin and IQGAP1 in endocrine cells

Men1 deletion and mutation causes multiple endocrine tumorigenesis (Lakhani *et al*., 2007). Similarly, IQGAP1 is widely expressed in various tissues. IQGAP1-null mutant mice develop gastric hyperplasia, lung adenoma/adenocarcinoma, and testicular atrophy or mineralization relative to wild-type animals of the same genetic background (Li *et al*., 2000). These observations are consistent with the notion that menin and IQGAP proteins may functionally link to the same pathway in the endocrine cells.

IQGAP1 lies in the midst of a complex signal transduction network that regulates cortical microfilaments organization, cell motility and cadherin-induced cell adhesion (Bashour *et al*., 1997; Kuroda *et al*., 1998). Several lines of evidence demonstrate that the interaction of IQGAP1 with menin contributes to the effects on cell adhesion and migration. First, menin increased β-cell aggression, which was attenuated by IQGAP1 knockdown (Figures 4a and b). Second, increasing menin concentration leads to a concomitant augmentation of IQGAP1, E-cadherin and β-catenin on the cell surface (Figures 3b and 4c). In contrast, menin ablation from islets *in vivo* decreased the accumulations of E-cadherin and β-catenin at the cell–cell contacts (Figure 4d). Third, menin forms supercomplex with IQGAP1 and β-catenin in β-cells (Figure 4e). Fourth, menin and Rac1 control the subcellular distributions of IQGAP1 in β-cells (Figures 3b and c). They competitively form complex with IQGAP1 *in vitro* and in cultured cells (Figures 3 and 6, Supplementary Figure S6). This result is in agreement with the previous discovery that reduction of Rac1–GTP level by TPA stimulation could decrease the Rac1–IQGAP1 complexes and increase the IQGAP1–β-catenin complexes (Fukata *et al*., 2001).

Regulation of cell motility and cell adhesion through menin–IQGAP1 pathway

Menin overexpression led to decreased cellular motility and increased cell–cell adhesion caused by recruitment of IQGAP1, E-cadherin and β-catenin to intercellular junctions. Paralleling these effects of menin overexpression were a reduction in the cytoplasmic levels of activated Rac1 (Figure 6d), a small G protein whose GTP-bound state and localization at membranes are positively regulated by IQGAP1, and which in turn regulates functional properties of IQGAP1 (Hart *et al*., 1996; Fukata *et al*., 2002; Mataraza *et al*., 2003; Watanabe *et al*., 2004). On the other hand, association of IQGAP1 with activated Rac1 was attenuated by menin structurally binding to IQGAP1 terminus (Figure 6e). These results implicate menin as an important regulator of IQGAP1 and Rac1, and by extension, the adhesion and motility of endocrine cells.

A previous model of intercellular adhesion stipulates specific regulatory roles for activated Rac1 and IQGAP1 (Noritake *et al*., 2005). The data on which the model is based on the binding of IQGAP1 to β-catenin abrogates binding of the β-catenin/E-cadherin complex to α-catenin and thus, leads to decreased adhesion. This IQGAP1-mediated inhibition of adhesion can be relieved, however, by binding of Rac1–GTP to IQGAP1, which displaces IQGAP1 from β-catenin (Kuroda *et al*., 1998). Other studies, however, show that activated Rac1 and Cdc42 interact with IQGAP1 and promote cell mobility and polarization (Mataraza *et al*., 2003; Watanabe *et al*., 2004, 2005). The result presented here indicated that strong adhesion in our β-cell lines was correlated with low, basal levels of Rac1–GTP, whereas weak adhesion was correlated with high Rac1–GTP levels and high cell mobility. These results strike us as different mechanisms to modulate IQGAP1 polarity in cell type-specific behavior.

Interplay between menin and IQGAP1 regulates IQGAP1 polarity function

Given that IQGAP1 functions in both cell adhesion and mobility, it would be asked what mechanism modulates the two activities in the same cell. IQGAP1 is both a downstream effector and an upstream activator of Cdc42, where active Cdc42 antagonizes IQGAP1 dissociation of the cell–cell contacts (Fukata *et al*., 1999; Lambert *et al*., 2002). Recently Cdc42 has been shown to inhibit IQGAP1's role in polarized secretion in β-cells or perhaps migration (Rittmeyer *et al*., 2008). Our results suggest that, at least in the Cdc42-deficient βHC9 cells, menin can replace the active Cdc42 and compete with Rac1 in a complex with IQGAP1, to increase IQGAP1–cadherin association at cell junctions (Figure 6e). In contrast, activation of Rac1 could increase IQGAP1–Rac1 activity in the cytoplasm and inhibit IQGAP1 association with the E-cadherin–β-catenin complex. Thus, menin and Rac1 competitive interactions with IQGAP1 drive IQGAP1 polarity functions at the cell–cell contacts versus its polarity functions at the leading edge of migrating cells (Figure 6e).

As menin represses Ras-mediated transformation in NIH 3T3 cells (Kim *et al*., 1999), and Rac1 is required for Ras-induced development of lung cancer in mice (Kissil *et al*., 2007), the results of this study may provide a new insight into how menin represses the oncogenic activity of Ras. On the other hand, our model may explain the loose association among islet cells in Men1 insulinoma (Bertolino *et al*., 2003). In epithelial cells, E-cadherin be involved in cell–cell adhesion, and loss of E-cadherin is a hallmark of tumor progression, cancer cell invasion and metastasis (Andl *et al*., 2006). Further work is required to biochemically decipher how menin inhibits Rac1 activation (Figure 6e).

Materials and methods

Constructs and cell lines

To generate pMX-Men1-TAP construct, the human *Men1* cDNA was subcloned in frame into *Bam-HI-Hind III* restriction sites of a pCTAP vector (Stratagene, La Jolla, CA, USA), and the resulting menin-TAP fragment was excised from this construct and cloned into the *Not1* and *BamH1* sites of retroviral plasmid, pMX-puro (Supplementary Figure S1A). pMX-Men1 was constructed by directly inserting human *Men1* cDNA fragment into pMX-puro at *Not1* and *BamH1* sites. All the retroviruses were packaged to infect

βHC9 cells as previously described (Chen *et al*., 2006). To stably overexpress wild-type menin, Mock cells were reinfected by pcDNA3-Men1 (La *et al*., 2004). A pLKO.1 lentiviral shRNA set targeting mouse IQGAP1 (RMM4534-NM_016721; Open Biosystem, Huntsville, AL, USA) was used to knockdown IQGAP1. All stable cell lines were created by antibiotic selection (puromycin for pMX-plasmids or G418 for pcDNA3.1-plasmids; Supplementary Figure S1). The cells were grown in Dulbecco's modified Eagle's medium (Mediatech Inc., Herndon, VA, USA) in the presence of 10% fetal bovine serum, 5% iron-supplemented calf serum (cosmic calf serum; Hyclone, Logan, UT, USA) and 1% penicillin–streptomycin (Invitrogen, Grand Island, NY, USA).

The mCherry-Rac1 vector was produced from an enhanced cyan fluorescent protein (eCFP)-Rac1 vector obtained from the lab of Dr Klaus Hahn. The eCFP coding region was excised from the eCFP-Rac1 vector and the mCherry coding region from an mCherry-C1 vector by *NheI* and *BsrGI* digestion (Shaner *et al*., 2004). β-Cell lines were transiently transfected using Lipofectamine 2000 Reagent (Invitrogen).

Fluorescence microscopy

Cells were fixed and stained with indicated antibodies as previously described (Yan *et al*., 2006b). The primary antibodies used in the study were purchased from companies as described in Supplementary Data. Texas Red-phalloidin (Invitrogen) was used to stain F-actin. The fluorescence was examined using a confocal laser scanning microscope (LSM510; Carl Zeiss, Oberkochene, Germany), and a series of images from 1-μm *YZ* sections were collected. Images were stacked using the LSM510 software and processed by Adobe Photoshop. Genotyping, excision of the floxed *Men1* locus and islet slide staining of mice were performed as describe earlier (Schnepp *et al*., 2006).

Purification of the tagged–menin complex and mass spectrometry analysis of the purified proteins

Mock and Men1-TAP cells (1.5×10^8) were separately lysed in cell lysis buffer (250 mM NaCl, 1 mM $MgCl_2$, 1 mM CaCl2, 50 mM Tris–HCl at pH 8.0, 0.5% NP-40, 5% glycerol, 2 × ethylenediaminetetraacetic acid (EDTA)-complete protease inhibitor cocktail (Roche, Mannheim, Germany). The lysates were quickly frozen in dry ice/ethanol slurry for 10 min, followed by incubation for 20 min in ice water. Two steps of purification were performed as recommended by the manufacturer (Stratagene). For analysis of protein complexes, a 1:15 volume of sample was separated in NuPAGE 4–12% Bis-Tris gel and visualized by silver stain (Silver Staining kit; Invitrogen). The other 1:15 volume was immunoblotted against menin antibody (Supplementary Figure S2). The remaining sample was fractionated in the same SDS gel and stained with colloidal Coommassie blue staining. Bands of interest were excised and analyzed by mass spectrometry.

Adhesion assays

Adhesion assays were performed essentially as described previously (Price *et al*., 2004) with certain modifications. Cells were detached with 1.5 mM-EDTA in phosphate-buffered saline (PBS; without calcium and magnesium) and diluted in serum-free medium. Cells (2×10^5 per well) were seeded to 96-well plates that had been precoated with either PBS, fibronectin (10 μg/ml) or goat antihuman immunoglobulin G Fc (20 μg/ml)/Fc-E-cadherin (2 μg/ml). After 20 min of incubation at room temperature and three washes, the adherent cells were counted from quadruplet wells.

Recombinant-binding assay

All affinity purification were essentially performed as described previously (Grohmanova *et al*., 2004; Le Clainche *et al*., 2007). Briefly, glutathione *S*-transferase (GST)-tagged IQGAP1 C-terminal fragments were expressed in *Escherichia coli* (DH5α) and induced with 0.1 mM isopropyl 1-thio-β-D-galactopyranoside at 28 °C for 16 h. The cells were harvested in lysis buffer (10 mM Tris–HCl, pH 8.0, 150 mM NaCl, 0.5 mM EDTA, 2 mM $MgCl_2$, 2 mM $CaCl_2$, 0.1% NP40), sonicated and centrifuged at 13 000 *g* for 20 min. The supernatants were purified on Glutathione Sepharose 4B (GE Healthcare, Uppsala, Sweden). For menin-binding assay, the purified GST-fusion proteins were incubated with 0.2 μg of menin for 1 h at 4 °C.

IP, affinity assays, small G protein affinity-binding assays and migration assays are described in Supplementary methods.

Acknowledgements

The parent clonal βHC9 insulin-secreting cells (Radvanyi *et al*., 1993) were obtained from the cell repository of the Diabetes Research Center at the University of Pennsylvania, with permission of Dr FM Matschinsky. We thank Dr Faming Zhang for his gifts of purified MBP-tagged menin and nontagged menin, Dr Martin A Schwartz for mutant human Rac1 vectors and Dr Ruth Kroschewski for the IQGAP1 C-terminal constructs (C1–C4). All confocal images and quantitative analyses of fluorescent intensity were conducted at the Biomedical Imaging Core Facility at the University of Pennsylvania. We thank Peter Blessington, Alicia Nelson, Hai Shen, Mercy Gohil and Elena Blagoi for their technical assistance. A special thanks to Dr Claudia Andl and Dr Margaret Chou for their stimulating discussions. This work was supported in part from NIH grants (R01-CA-100912 and R01-CA-113962 to XH, and R01- NS051746 to GSB), and a grant from the American Diabetes Association (7-07-RA-60 to XH).

References

Andl CD, Fargnoli BB, Okawa T, Bowser M, Takaoka M, Nakagawa H *et al*. (2006). Coordinated functions of E-cadherin and transforming growth factor beta receptor II *in vitro* and *in vivo*. *Cancer Res* **66**: 9878–9885.

Bai F, Pei XH, Nishikawa T, Smith MD, Xiong Y. (2007). p18Ink4c, but not p27Kip1, collaborates with Men1 to suppress neuroendocrine organ tumors. *Mol Cell Biol* **27**: 1495–1504.

Bashour AM, Fullerton AT, Hart MJ, Bloom GS. (1997). IQGAP1, a Rac- and Cdc42-binding protein, directly binds and cross-links microfilaments. *J Cell Biol* **137**: 1555–1566.

Bensenor LB, Kan HM, Wang N, Wallrabe H, Davidson LA, Cai Y *et al*. (2007). IQGAP1 regulates cell motility by linking growth factor signaling to actin assembly. *J Cell Sci* **120**: 658–669.

Bertolino P, Tong WM, Herrera PL, Casse H, Zhang CX, Wang ZQ. (2003). Pancreatic beta-cell-specific ablation of the multiple endocrine neoplasia type 1 (*MEN1*) gene causes full penetrance of insulinoma development in mice. *Cancer Res* **63**: 4836–4841.

Brandt DT, Marion S, Griffiths G, Watanabe T, Kaibuchi K, Grosse R. (2007). Dia1 and IQGAP1 interact in cell migration and phagocytic cup formation. *J Cell Biol* **178**: 193–200.

Chandrasekharappa SC, Guru SC, Manickam P, Olufemi SE, Collins FS, Emmert-Buck MR *et al*. (1997). Positional cloning of the gene for multiple endocrine neoplasia-type 1. *Science* **276**: 404–407.

Chen YX, Yan J, Keeshan K, Tubbs AT, Wang H, Silva A *et al*. (2006). The tumor suppressor menin regulates hematopoiesis and

myeloid transformation by influencing *Hox* gene expression. *Proc Natl Acad Sci USA* **103**: 1018–1023.

Crabtree JS, Scacheri PC, Ward JM, Garrett-Beal L, Emmert-Buck MR, Edgemon KA *et al*. (2001). A mouse model of multiple endocrine neoplasia, type 1, develops multiple endocrine tumors. *Proc Natl Acad Sci USA* **98**: 1118–1123.

Crabtree JS, Scacheri PC, Ward JM, McNally SR, Swain GP, Montagna C *et al*. (2003). Of mice and MEN1: insulinomas in a conditional mouse knockout. *Mol Cell Biol* **23**: 6075–6085.

Donnadieu E, Cefai D, Tan YP, Paresys G, Bismuth G, Trautmann A. (1992). Imaging early steps of human T cell activation by antigen-presenting cells. *J Immunol* **148**: 2643–2653.

Fukata M, Kuroda S, Nakagawa M, Kawajiri A, Itoh N, Shoji I *et al*. (1999). Cdc42 and Rac1 regulate the interaction of IQGAP1 with beta-catenin. *J Biol Chem* **274**: 26044–26050.

Fukata M, Nakagawa M, Itoh N, Kawajiri A, Yamaga M, Kuroda S *et al*. (2001). Involvement of IQGAP1, an effector of Rac1 and Cdc42 GTPases, in cell–cell dissociation during cell scattering. *Mol Cell Biol* **21**: 2165–2183.

Fukata M, Watanabe T, Noritake J, Nakagawa M, Yamaga M, Kuroda S *et al*. (2002). Rac1 and Cdc42 capture microtubules through IQGAP1 and CLIP-170. *Cell* **109**: 873–885.

Grohmanova K, Schlaepfer D, Hess D, Gutierrez P, Beck M, Kroschewski R. (2004). Phosphorylation of IQGAP1 modulates its binding to Cdc42, revealing a new type of rho-GTPase regulator. *J Biol Chem* **279**: 48495–48504.

Guru SC, Crabtree JS, Brown KD, Dunn KJ, Manickam P, Prasad NB *et al*. (1999). Isolation, genomic organization, and expression analysis of Men1, the murine homolog of the *MEN1* gene. *Mamm Genome* **10**: 592–596.

Guru SC, Goldsmith PK, Burns AL, Marx SJ, Spiegel AM, Collins FS *et al*. (1998). Menin, the product of the *MEN1* gene, is a nuclear protein. *Proc Natl Acad Sci USA* **95**: 1630–1634.

Hart MJ, Callow MG, Souza B, Polakis P. (1996). IQGAP1, a calmodulin-binding protein with a rasGAP-related domain, is a potential effector for cdc42Hs. *EMBO J* **15**: 2997–3005.

Huang SC, Zhuang Z, Weil RJ, Pack S, Wang C, Krutzsch HC *et al*. (1999). Nuclear/cytoplasmic localization of the multiple endocrine neoplasia type 1 gene product, menin. *Lab Invest* **79**: 301–310.

Hughes CM, Rozenblatt-Rosen O, Milne TA, Copeland TD, Levine SS, Lee JC *et al*. (2004). Menin associates with a trithorax family histone methyltransferase complex and with the hoxc8 locus. *Mol Cell* **13**: 587–597.

Jiang K, Sun J, Cheng J, Djeu JY, Wei S, Sebti S. (2004). Akt mediates Ras downregulation of RhoB, a suppressor of transformation, invasion, and metastasis. *Mol Cell Biol* **24**: 5565–5576.

Kim YS, Burns AL, Goldsmith PK, Heppner C, Park SY, Chandrasekharappa SC *et al*. (1999). Stable overexpression of MEN1 suppresses tumorigenicity of RAS. *Oncogene* **18**: 5936–5942.

Kissil JL, Walmsley MJ, Hanlon L, Haigis KM, Bender Kim CF, Sweet-Cordero A *et al*. (2007). Requirement for Rac1 in a K-ras induced lung cancer in the mouse. *Cancer Res* **67**: 8089–8094.

Kuroda S, Fukata M, Nakagawa M, Fujii K, Nakamura T, Ookubo T *et al*. (1998). Role of IQGAP1, a target of the small GTPases Cdc42 and Rac1, in regulation of E-cadherin-mediated cell–cell adhesion. *Science* **281**: 832–835.

La P, Schnepp RW, Petersen CD, Silva AC, Hua X. (2004). Tumor suppressor menin regulates expression of insulin-like growth factor binding protein 2. *Endocrinology* **145**: 3443–3450.

Lakhani VT, You YN, Wells SA. (2007). The multiple endocrine neoplasia syndromes. *Annu Rev Med* **58**: 253–265.

Lambert M, Choquet D, Mege RM. (2002). Dynamics of ligand-induced, Rac1-dependent anchoring of cadherins to the actin cytoskeleton. *J Cell Biol* **157**: 469–479.

Le Clainche C, Schlaepfer D, Ferrari A, Klingauf M, Grohmanova K, Veligodskiy A *et al*. (2007). IQGAP1 stimulates actin assembly through the N-WASP-Arp2/3 pathway. *J Biol Chem* **282**: 426–435.

Li S, Wang Q, Chakladar A, Bronson RT, Bernards A. (2000). Gastric hyperplasia in mice lacking the putative Cdc42 effector IQGAP1. *Mol Cell Biol* **20**: 697–701.

Lopez-Egido J, Cunningham J, Berg M, Oberg K, Bongcam-Rudloff E, Gobl A. (2002). Menin's interaction with glial fibrillary acidic protein and vimentin suggests a role for the intermediate filament network in regulating menin activity. *Exp Cell Res* **278**: 175–183.

Mataraza JM, Briggs MW, Li Z, Entwistle A, Ridley AJ, Sacks DB. (2003). IQGAP1 promotes cell motility and invasion. *J Biol Chem* **278**: 41237–41245.

Mataraza JM, Li Z, Jeong HW, Brown MD, Sacks DB. (2007). Multiple proteins mediate IQGAP1-stimulated cell migration. *Cell Signal* **19**: 1857–1865.

Mateer SC, McDaniel AE, Nicolas V, Habermacher GM, Lin MJ, Cromer DA *et al*. (2002). The mechanism for regulation of the F-actin binding activity of IQGAP1 by calcium/calmodulin. *J Biol Chem* **277**: 12324–12333.

Milne TA, Briggs SD, Brock HW, Martin ME, Gibbs D, Allis CD *et al*. (2002). MLL targets SET domain methyltransferase activity to *Hox* gene promoters. *Mol Cell* **10**: 1107–1117.

Milne TA, Hughes CM, Lloyd R, Yang Z, Rozenblatt-Rosen O, Dou Y *et al*. (2005). Menin and MLL cooperatively regulate expression of cyclin-dependent kinase inhibitors. *Proc Natl Acad Sci USA* **102**: 749–754.

Noritake J, Watanabe T, Sato K, Wang S, Kaibuchi K. (2005). IQGAP1: a key regulator of adhesion and migration. *J Cell Sci* **118**: 2085–2092.

Price LS, Hajdo-Milasinovic A, Zhao J, Zwartkruis FJ, Collard JG, Bos JL. (2004). Rap1 regulates E-cadherin-mediated cell–cell adhesion. *J Biol Chem* **279**: 35127–35132.

Radvanyi F, Christgau S, Baekkeskov S, Jolicoeur C, Hanahan D. (1993). Pancreatic beta cells cultured from individual preneoplastic foci in a multistage tumorigenesis pathway: a potentially general technique for isolating physiologically representative cell lines. *Mol Cell Biol* **13**: 4223–4232.

Ridley AJ. (2001). Rho family proteins: coordinating cell responses. *Trends Cell Biol* **11**: 471–477.

Rittmeyer EN, Daniel S, Hsu SC, Osman MA. (2008). A dual role for IQGAP1 in regulating exocytosis. *J Cell Sci* **121**: 391–403.

Schnepp RW, Chen YX, Wang H, Cash T, Silva A, Diehl JA *et al*. (2006). Mutation of tumor suppressor gene *Men1* acutely enhances proliferation of pancreatic islet cells. *Cancer Res* **66**: 5707–5715.

Shaner NC, Campbell RE, Steinbach PA, Giepmans BN, Palmer AE, Tsien RY. (2004). Improved monomeric red, orange and yellow fluorescent proteins derived from *Discosoma* sp. red fluorescent protein. *Nat Biotechnol* **22**: 1567–1572.

Taylor SJ, Shalloway D. (1996). Cell cycle-dependent activation of Ras. *Curr Biol* **6**: 1621–1627.

Watanabe T, Noritake J, Kaibuchi K. (2005). Roles of IQGAP1 in cell polarization and migration. *Novartis Found Symp* **269**: 92–101; discussion 101–105, 223–230.

Watanabe T, Wang S, Noritake J, Sato K, Fukata M, Takefuji M *et al*. (2004). Interaction with IQGAP1 links APC to Rac1, Cdc42, and actin filaments during cell polarization and migration. *Dev Cell* **7**: 871–883.

Yan J, Chen YX, Desmond A, Silva A, Yang Y, Wang H *et al*. (2006a). Cdx4 and menin co-regulate hoxa9 expression in hemato-poietic cells. *PLoS ONE* **1**: e47.

Yan J, Xu L, Crawford G, Wang Z, Burgess SM. (2006b). The forkhead transcription factor FoxI1 remains bound to condensed mitotic chromosomes and stably remodels chromatin structure. *Mol Cell Biol* **26**: 155–168.

Yokoyama A, Somervaille TC, Smith KS, Rozenblatt-Rosen O, Meyerson M, Cleary ML. (2005). The menin tumor suppressor protein is an essential oncogenic cofactor for MLL-associated leukemogenesis. *Cell* **123**: 207–218.

Supplementary Information accompanies the paper on the Oncogene website (http://www.nature.com/onc)

Supporting Information

Material and Methods

IQGAP1 polyclonal and monoclonal antibodies were generated as previously described (Mateer *et al.*, 2002). The other antibodies were purchased from BD Biosceinces [IQGAP1 (610611), Rac1 (610650), CDC42 (610928), Rho (610990), β-catenin (610153), and E-cadherin (610182)], Abcam [hnRNP U (ab20666)], Bethyl Laboratories, Inc. [menin (BL342)], Cell Signaling [β-actin (4967)], and Santa Cruz Biotechnology, Inc. [α Tubulin (sc-5286)].

Migration assays

A modified Boyden chamber assay was developed using HTS FluroBLok inserts (Becton Dickson). Cells were resuspended at a concentration of $2x10^5$ /ml cells in culture medium containing 1.5% serum and 500 µl of this suspension was plated per well in triplicate onto the upper chamber and allowed to attach for 4 h. Inserts were then transferred to wells containing 500 µl of 15% serum-containing medium in the lower chamber. Migration was allowed to proceed for 24 h at 37 °C. Migratory and non-migratory cells were trypsinized, counted and then transferred to wells containing normal culture medium and cultured for one day. For scratch wound assay, subconfluent cells were scraped using sterilizing 10-µl pipette tips, washed with PBS and cultured in normal medium. The cells were observed under a Nikon Eclipse TE 300 inverted microscop, and images were captured daily.

IP and affinity pull-down assay

For IP experiments, the cell lysate was prepared as described in purification of the tagged-menin complex (see Material and Methods). The precleared supernatants were aliquoted and immunoprecipitated with 1 µg of the indicated antibody or normal rabbit IgG at 4 °C for 3 hr. Protein A-sepharose or GammaBind Plus Sepharose (17-0886-01, GE Healthcare) was used to

collect the immunocomplex. For affinity pull-down assays, the recombinant His-tagged IQGAP1 N-terminal fragments (Bensenor *et al.*, 2007) were mixed with purified menin and/or GDP-/GTP-Rac1 and precipitated using Ni-NTA-agarose (Nickel) affinity beads (Qiagen). GDP-Rac1 and GTPγS Rac1 were loaded with their respective nucleotides in vitro using a Rac1 Activation Assay Kit (Upstate) following the provided protocol.

Small G protein affinity binding assays

Cells were grown to 80% confluence in 150 mm dish, starved overnight in 1.5% serum-containing medium, and recovered in normal medium for 30 min. The activity of Cdc42, Rac1 and Rho1 was determined by Rac1, Cdc42 or Rho activation Assay Kits (17-283, #AB4201, and 17-294, Upstate, Temecula, CA), respectively, based on the manufacturer's instructions.

Titles and legends to figures

Fig.S1 The diagram shows the generation of βHC9-derived cell lines. **(A)** βHC9-derived cell lines. **(B)** Comparison of morphology changes among sole retroviral infected mock cells, menin-coexpressing cells (Men1-TAP and Men1). Ectopic expression of menin in mock cells (mock+menin) partially increased aggregation of the infected cells. Approximately 75% of the mock+menin cells became round and clustered. Also seen in such cultures were cells with an intermediate morphology characterized by an overall round shape along with lamellipodium-like protrusions. Cells were cultured in flasks and photographed under inverted microscopy. **(C)** Immunoblot analyses of menin and IQGAP1 expression level.

Fig.S2 Various purification steps were examined by western blot using a menin-specific antibody. Compared with mock-infected cells (Mock), menin-expressing cells (Men1-TAP) expressed approximately two-fold greater levels of endogenous menin.

Fig.S3 Overexpression of Rac1 increases Rac1 activity. Men1-TAP cells were transiently transfected with mCherry-Rac1 or RFP-Rac1 (Q61L) vectors. The Rac1-GTP was harvested by Pak agarose (see Material and Methods). Samples were resolved by SDS/PAGE and probed with anti-Rac1 monoclonal antibody. Non-transfected Men1-TAP cells and RFP-Rac1 (Q61L) transfected cells were used as controls.

Fig.S4 IQGAP1 is crucial for cell-cell contact. IQGAP1 deletion reduces β-catenin and E-cadherin at cell junctions. βHC9 cells were infected with either IQGAP1 ShRNA or scrambled ShRNA lentiviruses, followed by confocal analyses of amount and distributions of IQGAP1, β-catenin and E-cadherin.

Fig.S5 Constitutively **a**ctive Rac1 abrogates menin inhibition of migration of ßHC9-derived cells. RFP-Rac1 (Q61L) was transiently expressed in Men1-TAP cells. After 6 hours of transfection, the cells were scratched and 24 hours later migratory cells were photographed. One of three assays was shown (n=3; ±S.D.).

Fig. S6. Menin inhibits binding of activated Rac1 to IQGAP1. **(A)** Ni-NTA agarose beads were used to pull down his-tagged IQGAP1 in the absence or presence of menin and/or Rac1. IQGAP1 (2μg), menin (0.2 μg) and Rac1 (1μg) were supplemented with bovine serum albumin (BSA). Thus, each 200 μl of reaction contained total of 3.2 μg proteins. **(B)** Co-IP assays showed higher levels of Rac1-IQGAP1 complex in mock cells compared to menin-expressing cells. Anti-mouse IgG (γ chain specific) peroxidase conjugate (Sigma, A3673) was used in immunoblot analyses. (**C**) The affinity of Rac1 to IQGAP1 was quantified as in (B). The amount of Rac1-bound IQGAP1 was normalized by the protein density from input IQGAP1 of mock cells.*, paired *t*-test, $P<0.05$. (D) Small Rho-GTPase assays. Total protein and GTP-form levels in whole cell lysates. The left panel showed comparisons among mock cells, Men1-TAP cells and Men1 cells. The right panel showed the difference between mock cells and re-expression of

menin in mock cells (mock+menin, Fig. S1A). **(E)** Total expression level of Cdc42 and Rac1. THP1 (human acute monocytic leukemia cell line) as a positive control.

Fig. S1

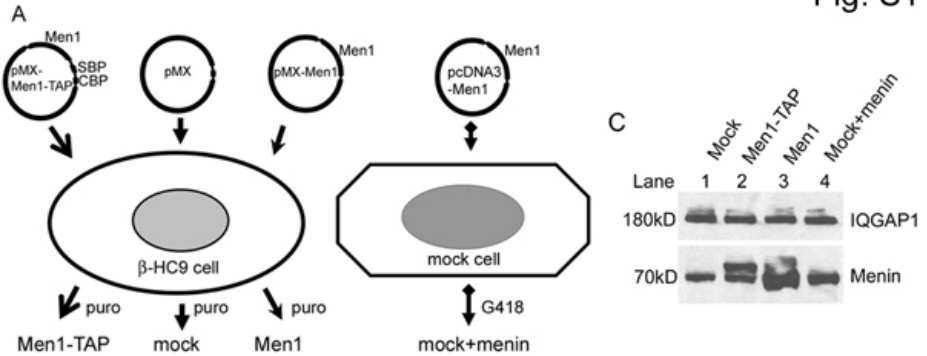
A
Men1
pMX-Men1-TAP
SBP
CBP
pMX
pMX-Men1
Men1
pcDNA3-Men1
Men1
β-HC9 cell
mock cell
puro
puro
puro
G418
Men1-TAP
mock
Men1
mock+menin
C
Mock
Men1-TAP
Men1
Mock+menin
Lane 1 2 3 4
180kD
IQGAP1
70kD
Menin

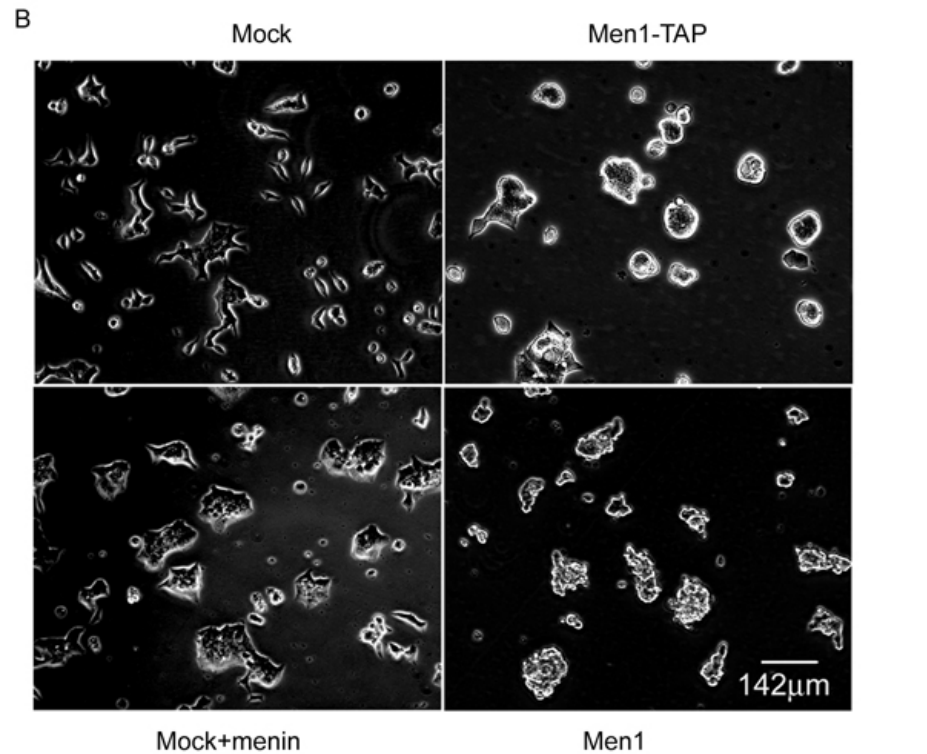
B
Mock
Men1-TAP
142μm
Mock+menin
Men1

Fig.S2

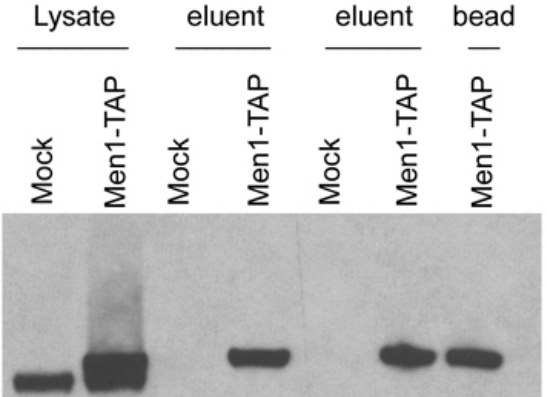
Lysate
SBP eluent
CBP eluent
CBP bead
Mock
Men1-TAP
Mock
Men1-TAP
Mock
Men1-TAP
Men1-TAP
75

Fig.S3

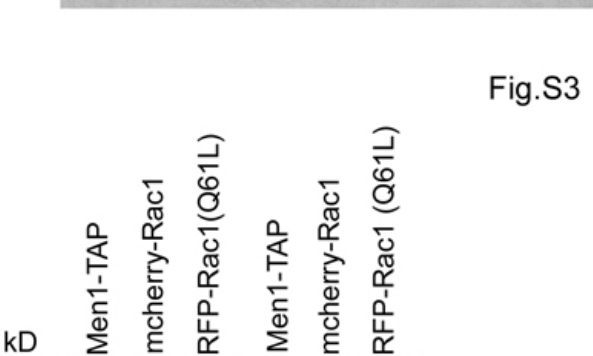
kD
Men1-TAP
mcherry-Rac1
RFP-Rac1(Q61L)
Men1-TAP
mcherry-Rac1
RFP-Rac1 (Q61L)
50
21
Exogenous
Endogenous
Total Rac1
Rac1-GTP

Fig. S4

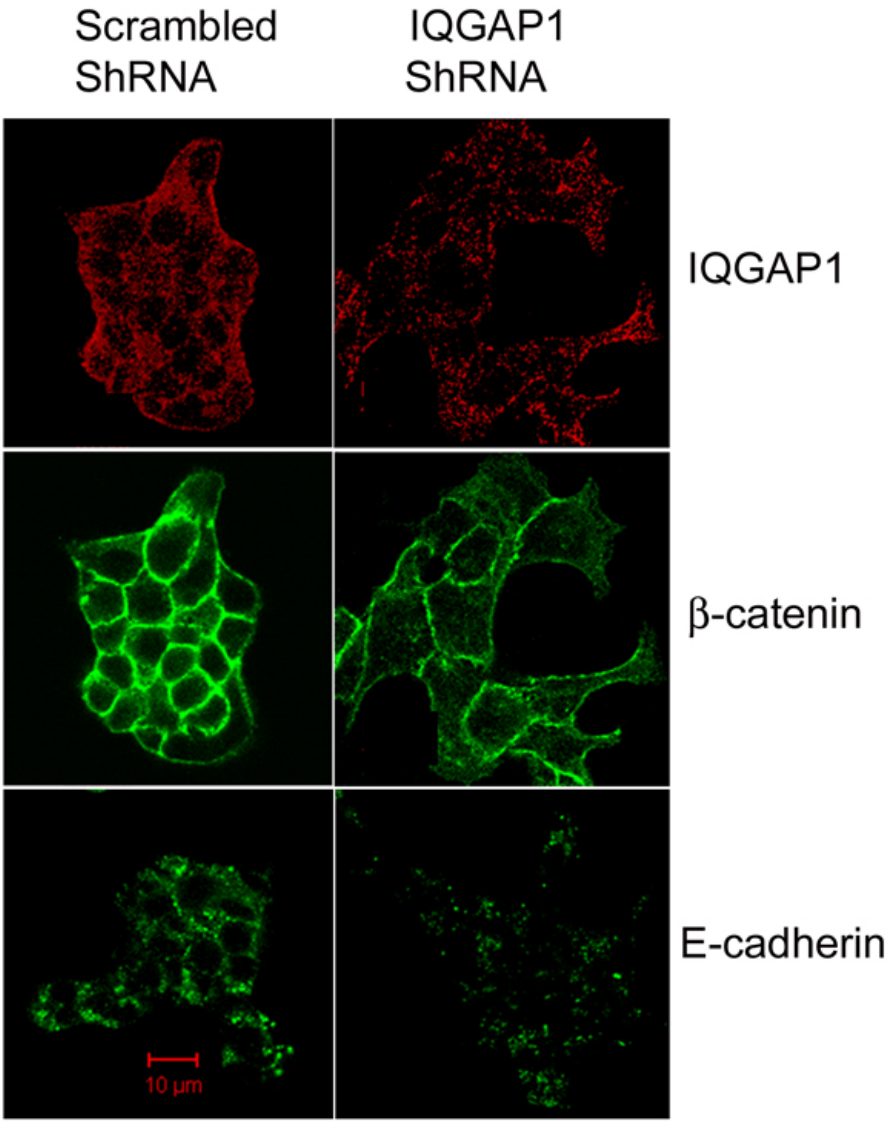
Scrambled ShRNA
IQGAP1 ShRNA
IQGAP1
β-catenin
E-cadherin
10 μm

Fig. S5

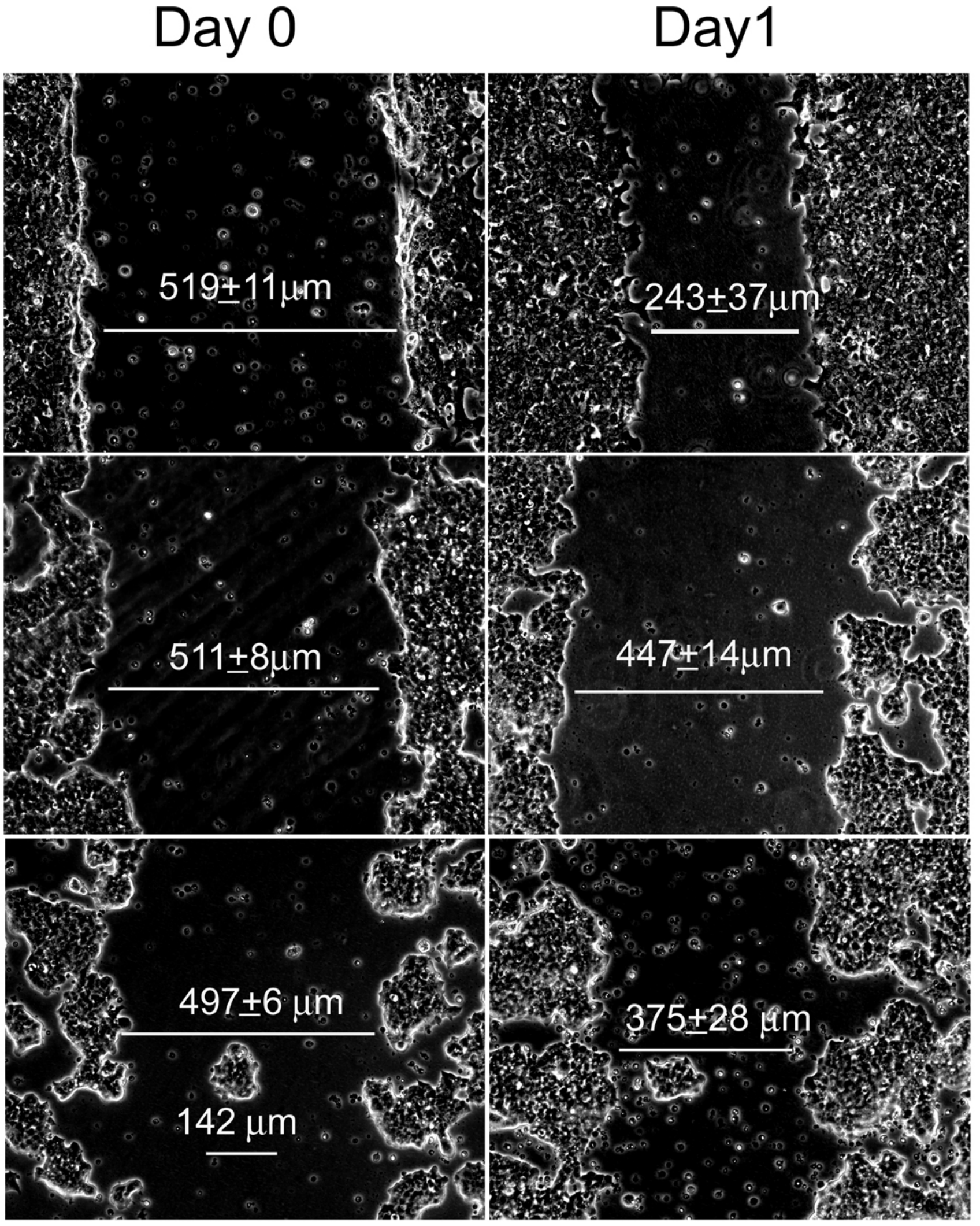
Day 0
Day1
519±11μm
243±37μm
Mock
511±8μm
447±14μm
Men1-TAP
497±6 μm
142 μm
375±28 μm
Men1-TAP
RFP-Rac1
(Q61L)

Fig. S6

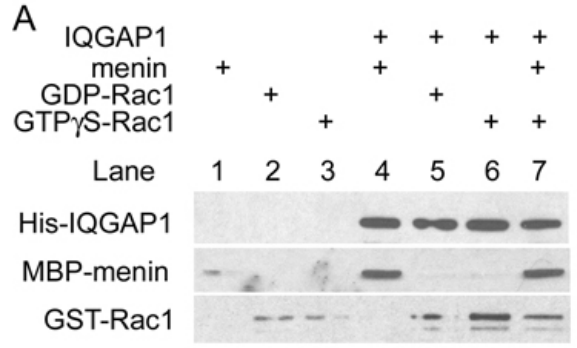
A
IQGAP1
menin
GDP-Rac1
GTPγS-Rac1
Lane 1 2 3 4 5 6 7
His-IQGAP1
MBP-menin
GST-Rac1

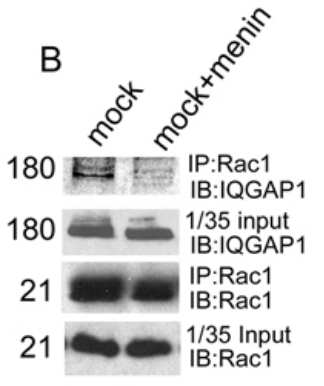
B
mock
mock+menin
180
IP:Rac1
IB:IQGAP1
180
1/35 input
IB:IQGAP1
21
IP:Rac1
IB:Rac1
21
1/35 Input
IB:Rac1

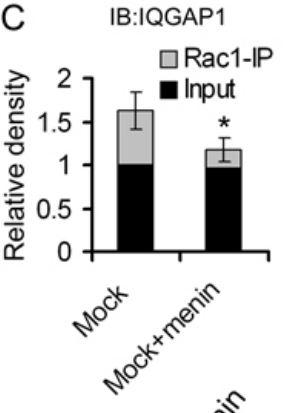
C
IB:IQGAP1
Rac1-IP
Input
Relative density
2
1.5
1
0.5
0
*
Mock
Mock+menin

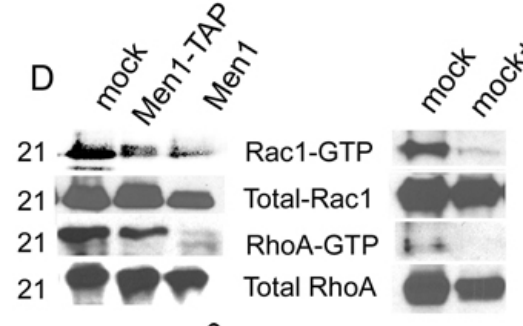
D
mock
Men1-TAP
Men1
mock
mock+menin
21
Rac1-GTP
21
Total-Rac1
21
RhoA-GTP
21
Total RhoA

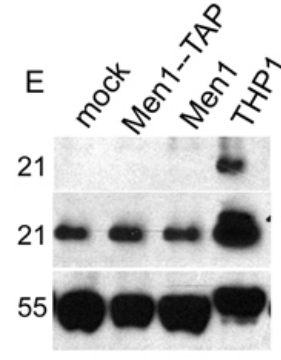
E
mock
Men1--TAP
Men1
THP1
21
Cdc42
21
Rac1
55
α-tubulin